CHAPTER VI

Mesomorphic, Optical, Dielectric and Visco-elastic Properties of Multi-component Mixtures

6.1. Introduction:

Liquid Crystal Displays (LCD's) have excellent properties, such as light weight, low power consumption, small thickness etc. and are the most popular flat panel displays at present. Vertically Aligned Liquid Crystal Displays (VA-LCDs) [1-4] are an attractive option for flat screen displays [5] because of very low transmission dark state [6] resulting in an excellent contrast ratio [7] and the intrinsic technology, which delivers perfect viewing angle characteristics. Thus VA-LCDs have become the most popular in direct-view display applications. They also show very reasonable performance in all other areas (e.g. driving voltage and response time) which has made them useful for large projection displays [8]. These types of LCD's require materials with negative dielectric anisotropy ($\Delta\varepsilon < 0$) [9-11]. In addition to negative dielectric anisotropy, these materials simultaneously require a wide nematic range (-40°C to 100°C), low birefringence ($\Delta n \sim 0.09$) [12], low bend elastic constant (K_{33}), and a low viscosity values ($\gamma_1 \sim 100$ mPas) [12]. No single liquid crystalline compound is suitable enough to meet the entire desired properties essential for a flat panel VA-LCD. As a result, LCD manufacturers require multicomponent liquid crystal mixtures with negative dielectric anisotropy. The problem of

careful formulation of multi-component mixtures with optimum values of the material properties has been undertaken in this work.

As mentioned in Chapter V, seven multi component mixtures (mixtures **A-G**) with negative dielectric anisotropy ($\Delta\varepsilon < 0$) have been prepared. Addition of a suitable dopant to the base mixture is a convenient technique to modify the physical properties of the final mixtures [13]. Another aspect that has to be taken into account during liquid crystal mixture selection is the voltage requirement to drive the cell. This comes down to the requirement that the dielectric anisotropy must be large enough [12]. Increasing the dielectric anisotropy may however affect the quality of the vertical alignment of the liquid crystal [14]. This can be alleviated by addition of small amounts of liquid crystal materials that have a small positive dielectric anisotropy (e.g. bicyclohexane). Therefore, from display point of view, preparation of suitable multicomponent mixtures and a detailed investigation into the dielectric, visco-elastic and other physical properties are of utmost importance.

In this chapter, the physical properties of seven multi-component mixtures (mixture **A-G**, Chapter V: Table 5.1) determined from optical birefringence (Δn), dielectric anisotropy ($\Delta\varepsilon$), bend elastic constant (K_{33}) and rotational viscosity measurements (γ_1) have been presented. Furthermore, the material properties of a few mixtures have been modified by the addition of appropriate dopants to meet the target specifications of VA mode mixtures. As the threshold voltage (V_{th}) is proportional to the square root of the ratio of the elastic constants and dielectric anisotropy [15, 16], mixtures with high values of the negative dielectric anisotropy and low values of bend elastic constant have been targeted. Lowering the value of V_{th} also results in consequent simplification of the driving electronics of the display applications. It is also imperative to determine the rotational viscosity coefficient (γ_1) of these materials as a function of temperature so as to obtain mixtures with lower values of γ_1 for fast switching VA mode displays. Additionally, the activation

energies (E_a) [17] have also been calculated for all of these multicomponent mixtures.

6.2. Physical properties of multi-component mixtures A-G:

6.2.1. Birefringence (Δn) and Orientational Order Parameter (OOP) measurements:

The temperature dependence of the principal refractive indices n_o and n_e, the mean value $\bar{n} = (n_e + 2n_o)/3$ and the refractive index in the isotropic phase (n_{iso}) at a wavelength of λ = 632.8 nm for the seven mixtures (mixture **A-G**), measured by thin prism technique [18, 19] are shown in Figures 6.1(a)-6.1(g). The ordinary refractive index (n_o) and the extraordinary refractive index (n_e) are plotted in Figures 6.2 and 6.3 respectively, against relative temperature (T_{NI}-T), in order to account for the different clearing temperatures.

The n_o values for mixture **A**, **B**, **C** and **G** (mixtures consist of compounds with bicyclohexane in the rigid core) are larger than that of **D**, **E** and **F** (mixtures consist of compounds with only laterally fluorinated terphenyl, biphenyl and tolanes). This is probably due to the fact that benzene rings are much more polarizable along the plane of the ring (because of the *delocalized π electrons*), whereas cyclohexane rings are less polarizable. Again, mixture **A** and **B** have the maximum values of n_o than the rest of the mixtures investigated throughout the entire nematic range. The tri-component mixtures (mixture **A** and mixture **B**) have same two pure components (laterally fluorinated terphenyl), only difference is found for the third component [16]. Mixture **A** consists of a pure compound with bicyclohexane in the rigid core and *ethylene* linking group, whereas mixture **B** consists of a pure compound with same rigid core but with an *ester* linking group. Ester linking group increases the molecular length and enhances the molecular polarizability and planarity and

so increases the nematic phase stability as well as the n_o values, whereas the immediate opposite effect is found for the *ethylene* linking group [20-22].

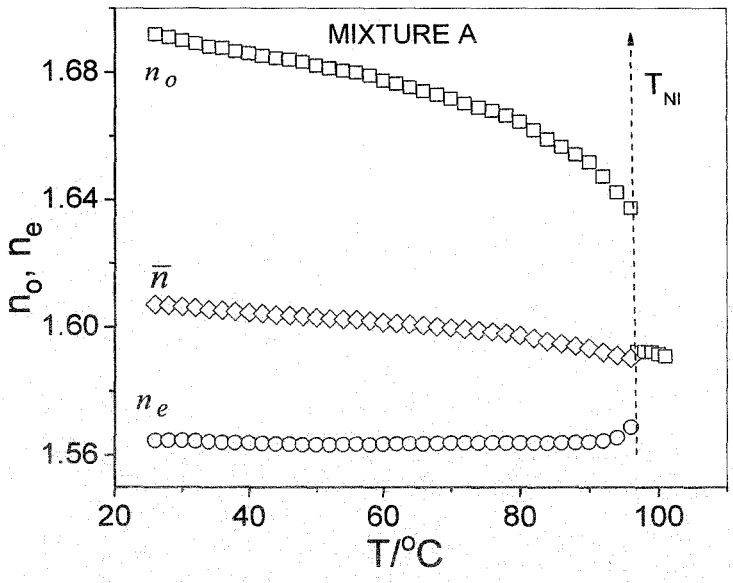

(a)

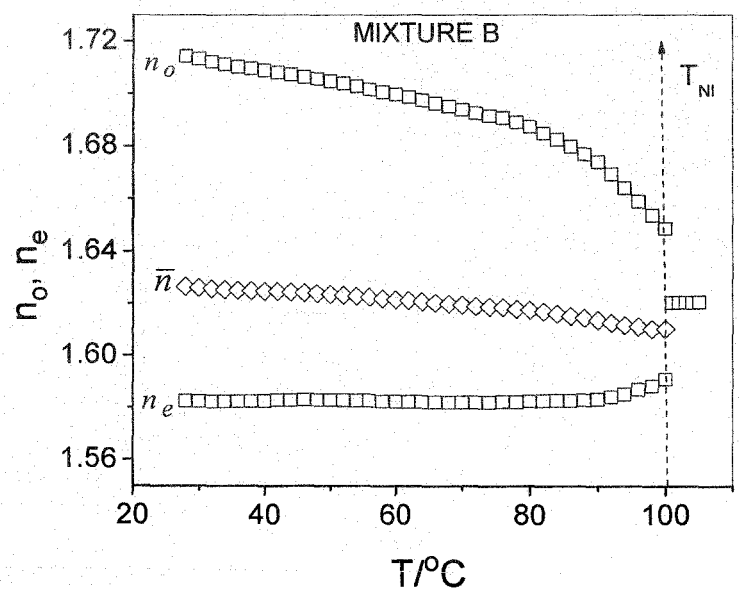

(b)

Figure 6.1. Experimental values of refractive indices n_o and n_e and mean value ($\bar{n}$) as a function of temperature for (a) mixture **A** and (b) mixture **B**. T_{NI} = nematic - isotropic phase transition temperature.

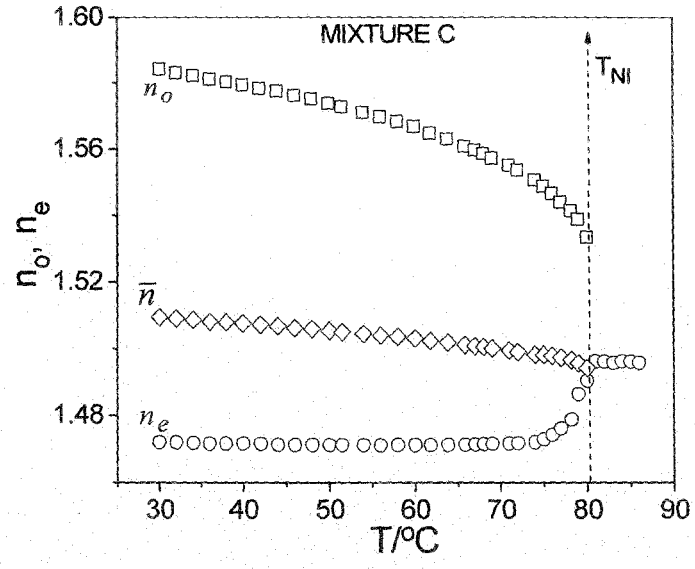

(c)

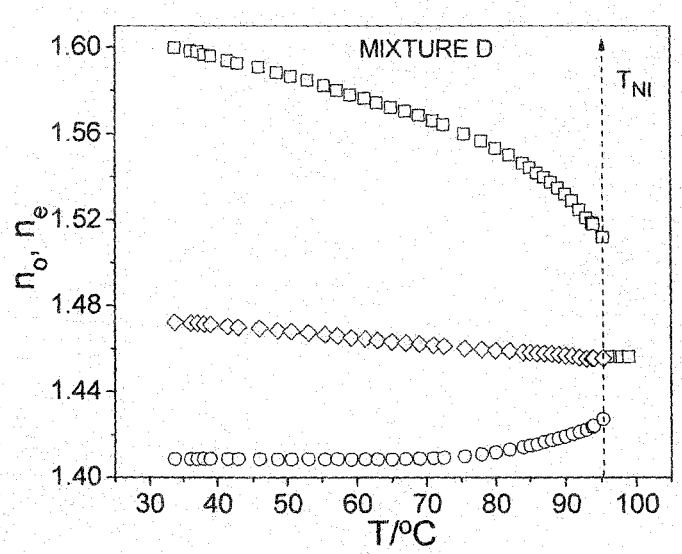

(d)

Figure 6.1. 'contd. Experimental values of refractive indices n_o and n_e and mean value ($\bar{n}$) as a function of temperature for (c) mixture **C** and (d) mixture **D**. T_{NI} = nematic - isotropic phase transition temperature.

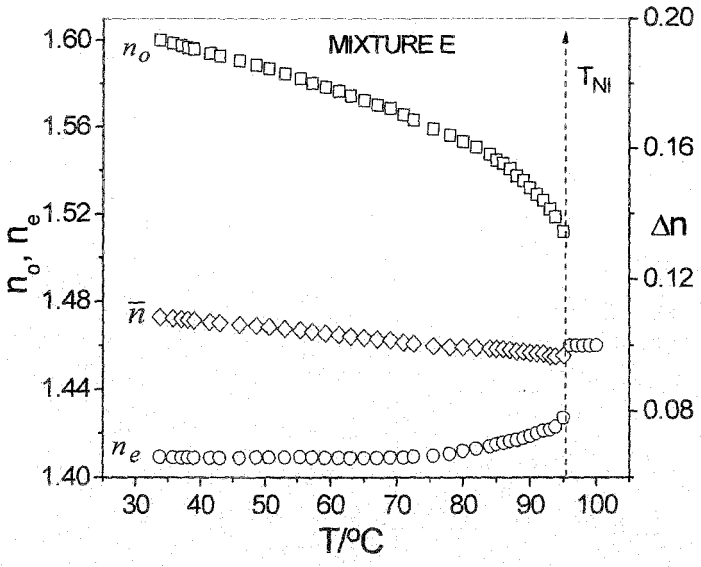

(e)

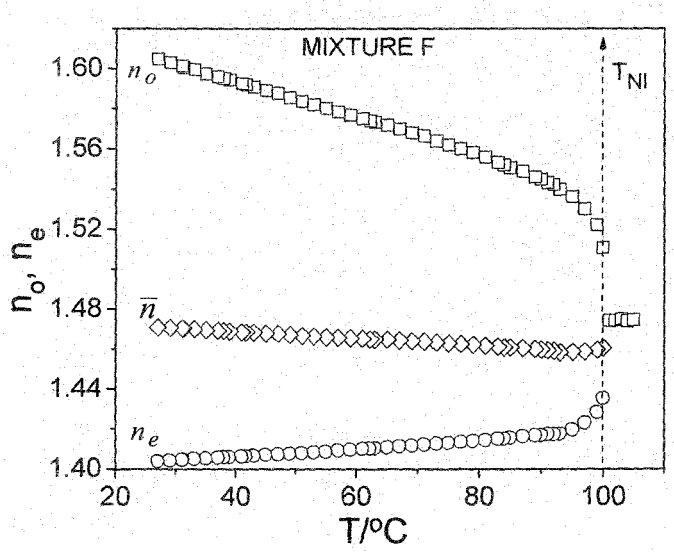

(f)

Figure 6.1. 'contd. Experimental values of refractive indices n_o and n_e and mean value ($\bar{n}$) as a function of temperature for (e) mixture **E** and (f) mixture **F**. T_{NI} = nematic - isotropic phase transition temperature.

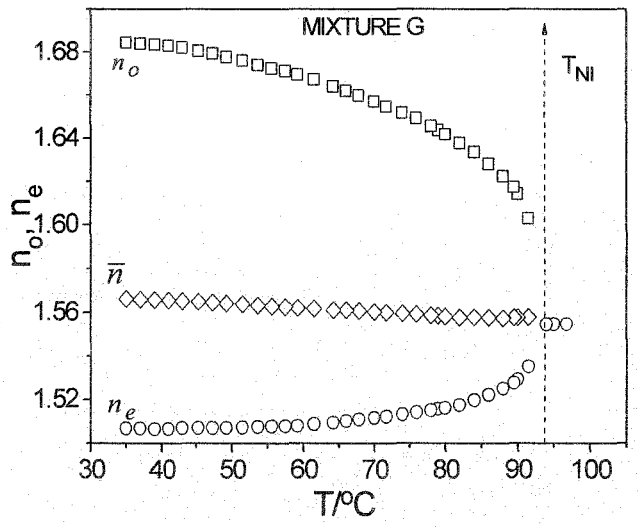

(g)

Figure 6.1. 'contd. Experimental values of refractive indices n_o and n_e and mean value ($\overline{n}$) as a function of temperature for (g) mixture **G**. T_{NI} = nematic - isotropic phase transition temperature.

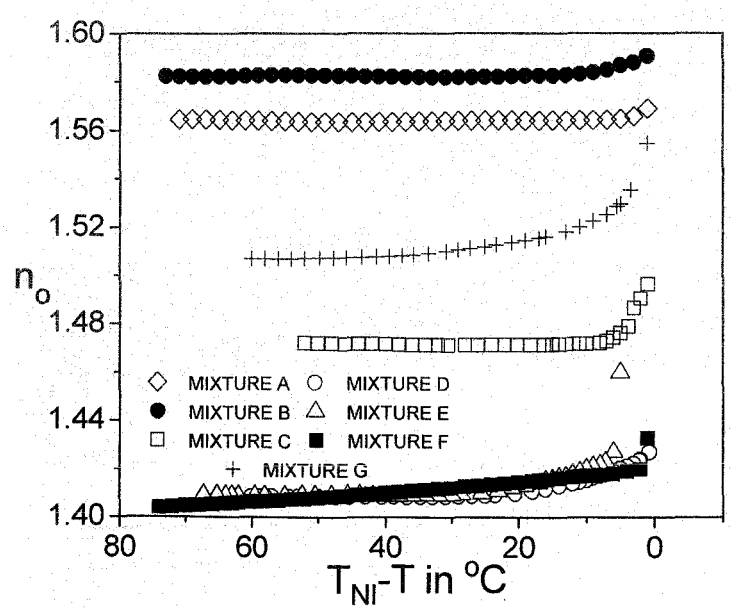

Figure 6.2. Ordinary refractive indices (n_o) as a function of relative temperature for different multicomponent mixtures (mixtures **A-G**). Key to symbols: ◊ mixture **A**, • mixture **B**, □ mixture **C**, o mixture **D**, Δ mixture **E**, ■ mixture **F** and + mixture **G**.

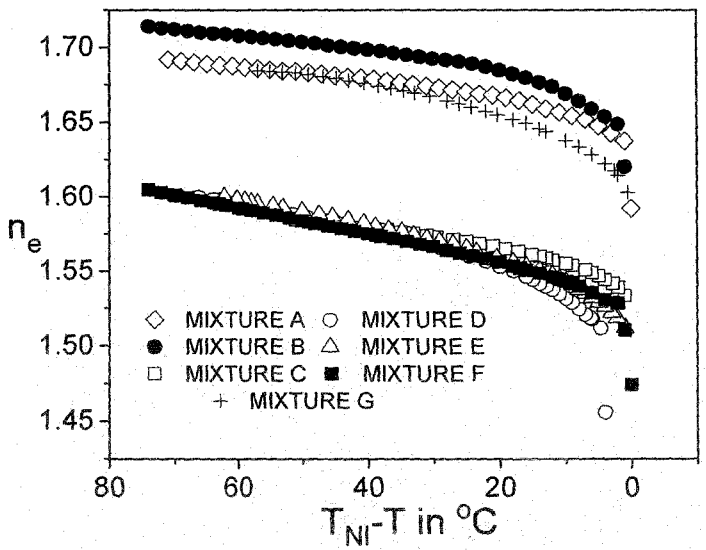

Figure 6.3. Extraordinary refractive indices (n_e) as a function of relative temperature for different multicomponent mixtures (mixtures **A-G**). Key to symbols: ◊ mixture **A**, • mixture **B**, □ mixture **C**, o mixture **D**, Δ mixture **E**, ■ mixture **F** and + mixture **G**.

Mixture **G** and mixture **C** consist of two *phenyl* bicyclohexane with an *alkoxy* terminal group, one *phenyl*-cyclohexane and one non-mesogenic compound, all these have *delocalized π electrons* in rigid core and hence n_o and n_e values are increased. However, the weight percentage of these compounds is greater in mixture **G**, as a result mixture **G** has greater value of n_o and n_e than mixture **B.** Mixture **D** consists of all laterally fluorinated bi-phenyl and tri-phenyl compounds. Two different laterally fluorinated tolanes has been added to mixture **D** as dopants to formulate mixture **E** and mixture **F** respectively. As one can observe that the tolane present in mixture **E** has one *acetylene* linking group (whereas the same present in mixture **F** has two *acetylene* linking groups) in between two aromatic core units, which maintains the linearity of the molecule and extends the molecular length and enhances longitudinal polarizability, and hence the nematic phase stability is significantly enhanced [20]. The effect of lateral flurosubstituted pure compounds is more in

transverse direction in comparison to longitudinal direction. It may be due to the dipole-dipole interaction of the polar fluorine molecules perpendicular to the molecular long axis.

Comparison of the ordinary (n_o) and extraordinary (n_e) refractive indices in the nematic phase of all the mixtures studied at T_{NI}-T = 10°C is shown below:

n_o: **B>A>G>C>E~F>D**

n_e: **B>A>G>C>E>D~F**

Figure 6.4 illustrates the results of the temperature dependence of the birefringence ($\Delta n=n_e-n_o$) of the seven mixtures (mixture **A-G**) investigated. It may be noted that the birefringence of the two tricomponent systems (mixture **A** and mixture **B**) are almost identical and show normal temperature dependence and are found to be around 0.12 and 0.13 respectively at 20°C (Figure 6.4) which is fairly good for VA mode LCDs [16]. Interestingly, among the seven mixtures investigated, the five component mixture (mixture **C**) showed lower birefringence values ($\Delta n \sim 0.11$ at T = 20°C) and also lower clearing temperature [15] which is close to the target specification for VA mode mixtures of around 0.08 using a cell gap of the LCD device to be around 4 μm [12]. All the mixtures **D-G** exhibit moderately high birefringence, for example, the value of Δn was in the range 0.18-0.20 at T = 20°C. The birefringence value for mixture **D** is found to be around 0.19 at 20°C which is slightly higher than the targeted value. From the Figure 6.4, it is observed that the Δn values are around 0.18 for both mixtures **E** and **F**, while for mixture **G** the value is around 0.19. An explanation might be given in the following way that the greater percentage of biphenyl and terphenyl components (and also the highly polar fluorine in the lateral position) leads to enhanced birefringence through the elongated π–electron conjugation system of the entire rigid core of the molecules than other mixtures studied. An inspection of Figure 6.4 reveals

that compounds of high birefringence as components of the multi-component mixtures enhance the overall birefringence (Δn) value.

Comparison of the Δn values in the nematic phase of all the mixtures studied at T_{NI}-T = 10°C has been found to be the following:

Δn: **D~E>F>G>A~B>C**

It is to be noted from the ascending order of n_o and n_e that they show exactly an opposite trend than the ascending order of Δn. This is due to the fact that the temperature variation of n_e is much more pronounced than the temperature variation of n_o throughout the mesomorphic range and also near the vicinity of the nematic to isotropic phase transition.

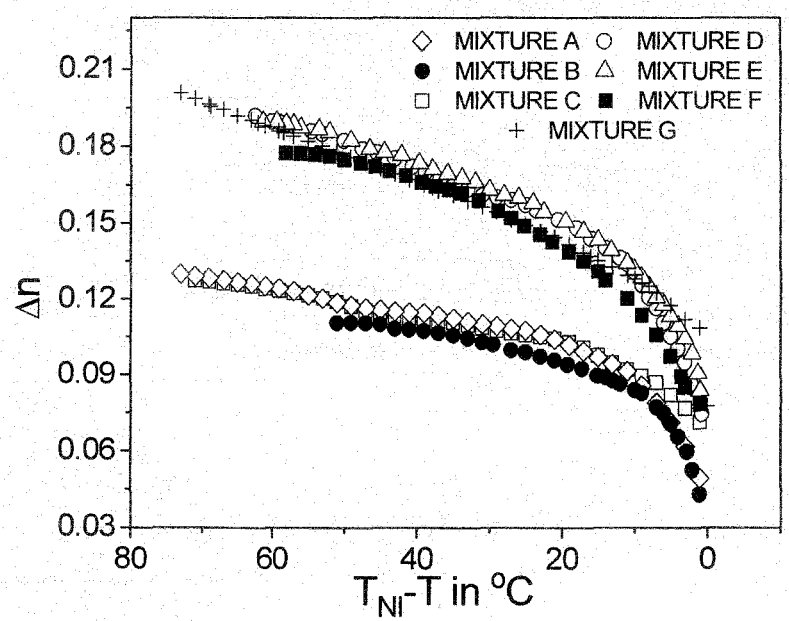

Figure 6.4. Birefringence (Δn) as a function of relative temperature for different multicomponent mixtures (mixtures **A-G**). Key to symbols: ◊ mixture **A**, • mixture **B**, □ mixture **C**, o mixture **D**, Δ mixture **E**, ■ mixture **F** and + mixture **G**.

The optical birefringence (Δn) obtained from thin prism technique was utilized to determine the temperature variation of the Orientational Order Parameter (OOP) in the liquid crystalline phases of these compounds. The

experimental temperature dependence of Δn in the nematic phase was fitted to the form

$$\Delta n = \Delta n_0 (1 - \frac{T}{T*})^{\beta} \tag{6.1}$$

where, T is the absolute temperature and T*, Δn_0 and β are fitting parameters by Haller's extrapolation method [23, 24]. This procedure is equivalent to the extrapolation of Δn to the temperature of absolute zero. The temperature dependent birefringence is related to the order parameter as:

$$< P_2 >= \frac{\Delta n}{\Delta n_0} \tag{6.2}$$

The Δn_0 value was determined in the nematic phase for all the multicomponent mixtures and was used to calculate the order parameter. The order parameters determined in this way for all the mixtures are shown in Figure 6.5.

It is to be noted that the typical procedure for the evaluation of the long range order parameter from optical method require the measurement of the ordinary and extraordinary refractive indices as well as the density data. In such cases, using these three measured quantities, either the standard Vuk's isotropic model [25] or the Neugebauer's relations based on the anisotropy of the internal field [26] are adopted to determine the principal polarizabilities parallel and perpendicular to the molecular long axes and hence, the anisotropy of the molecular polarizabilities (Δα) can be calculated. The normalized polarizability ($\Delta\alpha_o$) for perfectly order crystal is determined from the well-known Haller's extrapolation procedure and the order parameter is calculated from the ratio $\Delta\alpha/\Delta\alpha_0$. According to de Jue [17], the variation of density (ρ) over the nematic range is usually small and the temperature dependence of Δn gives a good indication of the variation of the order parameter with temperature. Kuczynski *et al.* [27] have also shown that the order parameter

determined directly from birefringence measurements are consistent with the $\langle P_2 \rangle$ values calculated from the polarizability data. Therefore in the present case, equation 6.2 has been fitted for all the mixtures considering the values of Δn in the nematic phase.

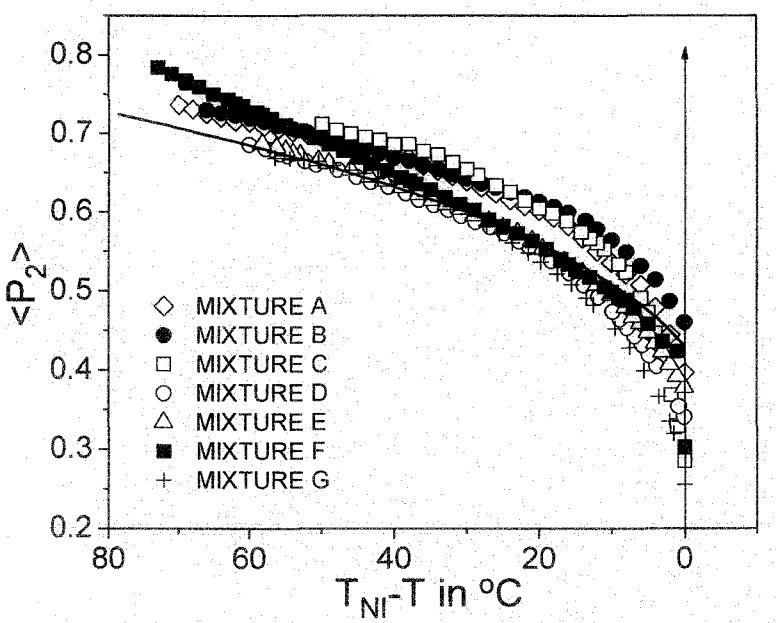

Figure 6.5. Order parameter ($\langle P_2 \rangle$) as a function of relative temperature for different multicomponent mixtures (mixtures **A-G**). Key to symbols: ◊ mixture **A**, • mixture **B**, □ mixture **C**, o mixture **D**, Δ mixture **E**, ■ mixture **F** and + mixture **G**. ---- line indicates the theoretically fitted MS curve. ↑ indicates nematic to isotropic transition (T_{NI}).

From Figure 6.5 it is observed that at room temperature the order parameter ($\langle P_2 \rangle$) [28-32] values are quite high for mixtures **A-C** and **F** (values are around 0.8), while for the rest mixtures (mixture **D**, **E** and **G**) order parameter values are quite low (values vary from 0.61-0.67), which implies that mixtures **A-C** and **F** are more ordered in the nematic phase than mixtures **D**, **E** and **G**. The reason lies in the number of components and also the nature of the pure compounds present in the mixtures. The lateral substituents in the pure compounds are larger and reasons into a proportionate reduction in the nematic

phase stability. It results into a reduction in the $<P_2>$ values. On the other hand lowering the number of the lateral substituents results in greater nematic phase stability [20, 21] and as a result higher $<P_2>$ values are obtained.

The variation of the fitted parameters (Δn_0, T* and β) from Haller's extrapolation method are listed in Table 6.1.

Table 6.1. Extrapolated birefringence at the absolute zero temperature (Δn_0), T*, exponent (β) for mixtures **A-G**.

Mixture Name	Δn_0	T* in K	β
A	0.173±0.002	372.1±0.9	0.19±0.007
B	0.178±0.002	374.7±0.4	0.19±0.006
C	0.157±0.001	352.9±0.2	0.17±0.002
D	0.278±0.002	367.7±0.5	0.21±0.004
E	0.277±0.002	367.9±0.3	0.21±0.003
F	0.256±0.004	372.0±0.7	0.19±0.009
G	0.265±0.004	362.3±0.8	0.20±0.008

6.2.2. Dielectric permittivity measurements:

The magnitude of the dielectric anisotropy ($\Delta\varepsilon$) directly determines the strength of interaction of the liquid crystalline material with an applied electric field, and therefore has a major influence on threshold voltage (V_{th}).

For comparison of the dielectric properties of the different mixtures (mixtures **A-G**), the dielectric parameters ($\varepsilon_{\parallel}$, $\varepsilon_{\perp}$), their ratio ($\varepsilon_{\perp}/\varepsilon_{\parallel}$) and the dielectric anisotropy ($\Delta\varepsilon$) have been plotted as a function of relative temperature (T_{NI}-T) and are shown in Figures 6.6-6.9 respectively.

The electron attractive group (e.g. CN, F) with large electro-negativity if substituted along the perpendicular direction to the molecular long axis effectively increases the transverse dielectric permittivity ($\varepsilon_{\perp}$). The most promising candidates for increasing the dielectric constants ($\varepsilon_{\parallel}, \varepsilon_{\perp}$) are liquid crystalline materials with 2, 3-difluoro benzene blocks [33]. The small van der

Waals volume of the fluorine atom (V_r = 5.8 Å) , large electro negativity (~ - 3.98) [34], relatively small dipole moment (1.47 D) lead to materials of relatively low viscosity and weak to moderately strong negative dielectric anisotropy in the nematic phase. If liquid crystalline mixtures consisting of compounds with fluorine in a lateral position with respect to the molecular long axis are prepared, the resultant dipole moment perpendicular to the long molecular axis is enhanced. As a result relatively larger values of the dielectric anisotropy ($-1 > \Delta\varepsilon > -3$) are induced, which promotes a lower value of threshold voltage (V_{th} = 2~3 volt, which is essential for display devices).

As observed from Figure 6.6 and 6.7 the dielectric constant in the perpendicular direction ($\varepsilon_\perp$) is much higher for mixtures with nine (mixture **D**), ten (mixture **E** and **F**) and fifteen (mixture **G**) components. The number of laterally fluorosubstituted terphenyl compounds is higher in those mixtures and mixture **E**, **F** and **G** also contains laterally fluorosubstituted phenyl-tolanes. These compounds posses unsaturated π bonds and contributes towards lower values of dielectric constant along the molecular long axis ($\varepsilon_\parallel$) and as a result the dielectric anisotropy is increased [21, 22]. However, mixtures **A**, **B** and **C** show lower values of dielectric constants along the perpendicular direction ($\varepsilon_\perp$) with respect to the molecular long axis. Mixtures **A** and **B** comprise of only two laterally fluorinated terphenyl derivative along with a bicyclohexane compound (which is different for **A** and **B**) [16]. Mixture **C** consists of a terphenyl derivative, two laterally fluorinated phenyl bicyclohexane, one phenyl cyclohexane compound and one non-mesogenic compound [15]. As a result for these three mixtures (mixture **A**, **B**, **C**), $\varepsilon_\perp$ is much lower in comparison to the rest of the mixtures ($\varepsilon_\perp$ values ranging from 4 to 5.5). It is found that the permittivity values along the molecular long axis ($\varepsilon_\parallel$) are nearly the same throughout their mesomorphic range for mixtures **C**, **B** and **G** and also lower than other mixtures. These mixtures contain pure compounds with bicyclohexane in rigid core and it is well known that cyclohexanes has non

planar structure [20] which contributes less in the molecular long axis resulting in decreasing values of $\varepsilon_{\parallel}$. But surprisingly, mixture **A** exhibits lowest dielectric permittivity values among all of the mixtures (Figure 6.6). This may be due to the fact that in mixture **A** there is a non-polar *ethylene* linking group and it has been found that compounds with *ethylene* group when present in mixtures suffer from poor stability, destroying the liquid crystalline properties [20, 21].

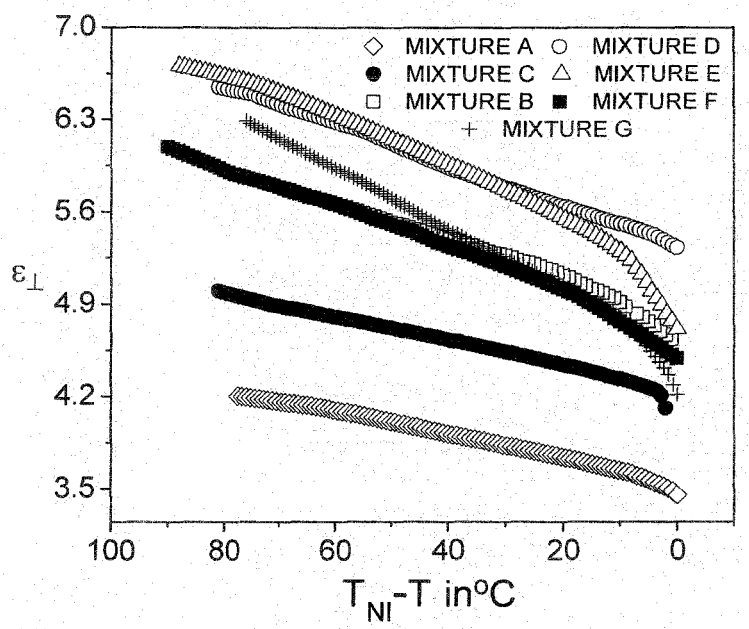

Figure 6.6. Dielectric constant ($\varepsilon_{\perp}$) as a function of relative temperature for different multicomponent mixtures (mixtures **A-G**). Key to symbols: ◊ mixture **A**, • mixture **B**, □ mixture **C**, o mixture **D**, Δ mixture **E**, ■ mixture **F** and + mixture **G**.

Mixture E shows highest values of $\varepsilon_{\perp}$ and mixture D shows highest values of $\varepsilon_{\parallel}$. Lowest values of $\varepsilon_{\perp}$ and $\varepsilon_{\parallel}$ are found for mixture A. Intermediate values of $\varepsilon_{\perp}$ and $\varepsilon_{\parallel}$ are found for rest of the mixtures. As the number of component increases the value of $\varepsilon_{\perp}$ and $\varepsilon_{\parallel}$ also increases. Tri-component mixtures (mixture **A** and **B**) have lower values of $\varepsilon_{\perp}$ and $\varepsilon_{\parallel}$ and mixtures **D-G** have higher values of $\varepsilon_{\perp}$ and $\varepsilon_{\parallel}$. Mixture **C** has moderate values of $\varepsilon_{\perp}$ and $\varepsilon_{\parallel}$.

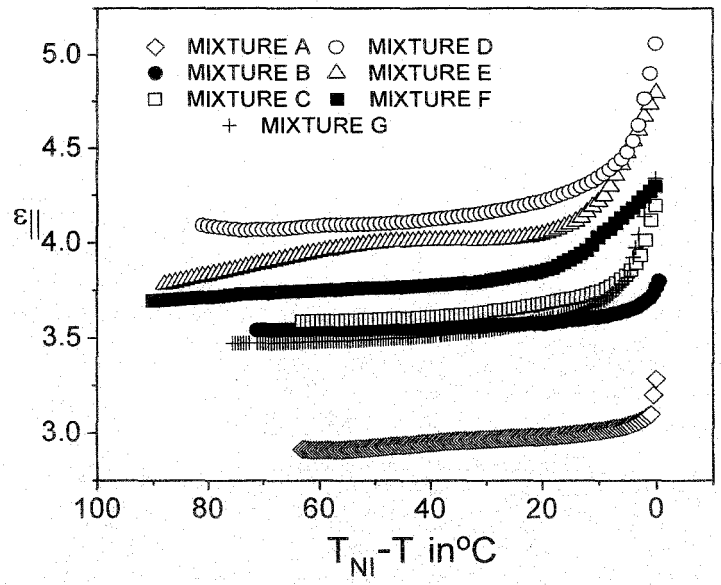

Figure 6.7. Dielectric constant ($\varepsilon_{\|}$) as a function of relative temperature for different multicomponent mixtures (mixtures **A-G**). Key to symbols: ◊ mixture **A**, • mixture **B**, □ mixture **C**, o mixture **D**, Δ mixture **E**, ■ mixture **F** and + mixture **G**.

In most displays the ratio of $\Delta\varepsilon$ to the perpendicular dielectric constant ($\varepsilon_{\perp}$) is very important [35]. A small ratio of $\Delta\varepsilon/\varepsilon_{\perp}$ is usually desirable, thus materials with a large $\Delta\varepsilon$ (to lower V_{th}) and $\varepsilon_{\perp}$ are needed. This is difficult to accomplish and therefore the $\varepsilon_{\perp}$ of a mixture is often increased by materials with a large negative dielectric anisotropy. To increase $\Delta\varepsilon$, more than one polar group can be considered [21, 22]. The final $\Delta\varepsilon$ value is determined by the vector sum of the total dipole moments. The magnitude of $\Delta\varepsilon$ and polar group type of an LC mixture affects the threshold voltage, operating voltage, power consumption, resistivity and viscosity. With this similar objective (to increase $\Delta\varepsilon$) mixture **D** with nine laterally fluorinated bi-phenyl and tri-phenyl have been prepared and modified into mixture **E** and **F** by addition of laterally fluorinated tolanes (again possessing high negative $\Delta\varepsilon$). Fluorines in lateral position traps π electrons resulting in a higher value of $\varepsilon_{\perp}$ (shown in

Figure 6.6). The ratio of dielectric constants ($\varepsilon_\perp/\varepsilon_\parallel$) for mixtures **A-G** are plotted in Figure 6.8. For mixture **G** the ratio has the highest value, which implies that along parallel and perpendicular direction the variation of dielectric constants are maximum in comparison to other mixtures. For mixture **A** and **B** this ratio has the lowest value which implies that for these two mixtures there is no major change in the values of permittivities in two directions and as a obvious result the $\Delta\varepsilon$ values are low for these mixtures in comparison to other mixtures.

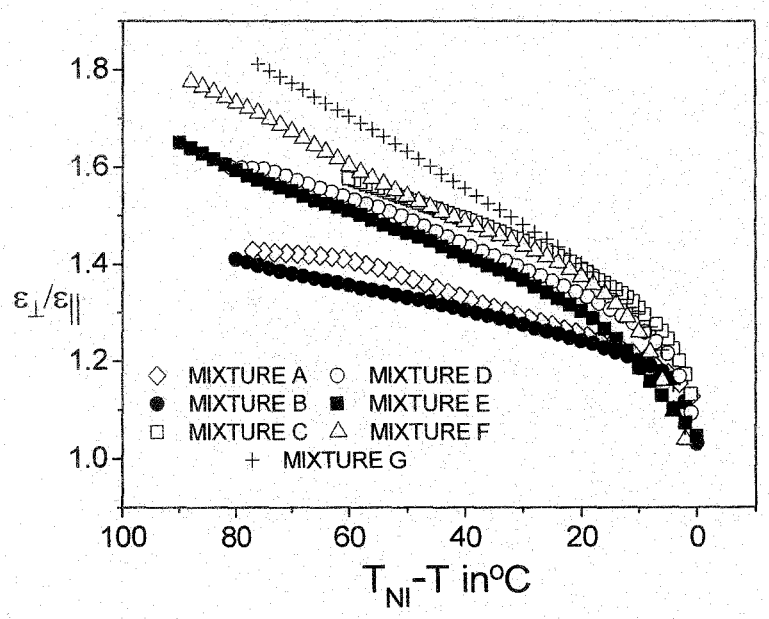

Figure 6.8. Ratio of dielectric constants ($\varepsilon_\perp/\varepsilon_\parallel$) as a function of relative temperature for different multicomponent mixtures (mixtures **A-G**). Key to symbols: ◊ mixture **A**, • mixture **B**, □ mixture **C**, o mixture **D**, Δ mixture **E**, ■ mixture **F** and + mixture **G**.

From the temperature dependence of dielectric anisotropy ($\Delta\varepsilon$) data for all the mixtures (as shown in Figure 6.9) it is observed that the dielectric anisotropy, $\Delta\varepsilon$, for mixture **B** is slightly higher than those obtained from **A** and its value is about −1.4 at around 20°C [16]. For mixture **C** the $\Delta\varepsilon$ value is around −1.0 at 20°C [15], which are somewhat low for VA mode displays.

Therefore there is a scope for further improvement regarding this parameter. The dielectric anisotropy (Δε) value for mixture **D** is moderately good (–2.42 at 20°C), while for mixture **E** it has increased to a value of –2.5 at around 20°C and it has a distinctly higher value for mixture **F**. The value reaches to –3.0 at around 20°C for mixture **F**. For the fifteen component mixture (mixture **G**), the Δε value is –2.6 at 20°C.

Comparison of the Δε in nematic phase of all the mixtures studied at T_{NI}–T = 10°C is shown below:

Δε G>F>D>E>B>A>C

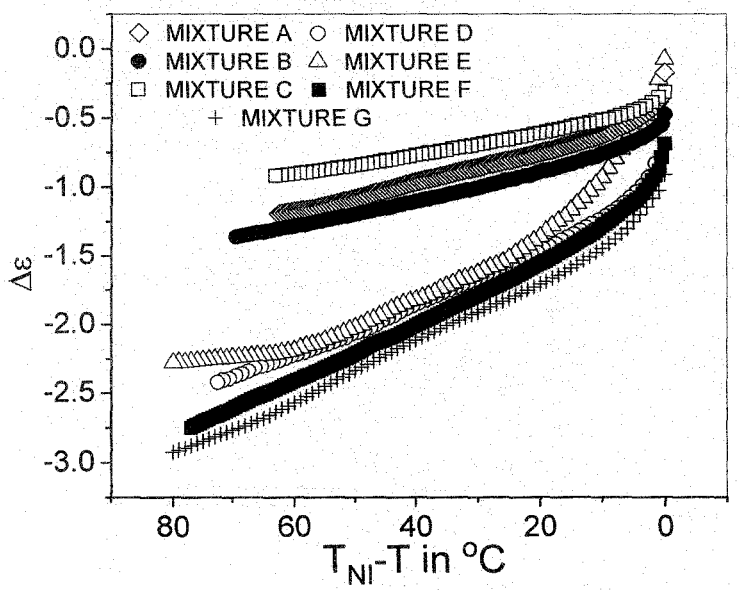

Figure 6.9. Dielectric anisotropy (Δε) as a function of relative temperature for different multicomponent mixtures (mixtures **A-G**). Key to symbols: ◊ mixture **A**, • mixture **B**, □ mixture **C**, o mixture **D**, Δ mixture **E**, ■ mixture **F** and + mixture **G**.

6.2.3. Bend elastic constant (K_{33}) measurements:

In Liquid Crystal Displays the electric or magnetic forces determine the static deformation pattern of a liquid crystal. On applying an external force (such as an electric field), the internal structure of the liquid crystalline material changes, and the elastic coefficients determine how the molecules reacts

through the restoring torque. The threshold voltage (V_{th}) depends on the dielectric anisotropy ($\Delta\varepsilon$) of liquid crystalline materials and also on its elastic behaviour. Higher values of dielectric anisotropy require low threshold voltages and therefore make lower values of bend elastic coefficients (K_{33}). The threshold voltage (V_{th}) of the cell in vertically aligned mode display is designed to be 2~3 V, and is determined by the choice of the liquid-crystal materials to be used. The maximum operating voltage, or the peak amplitude of the data signal of the display, is about 7~8 V [12]. This low voltage and the low current due to the high resistance of the liquid crystal material contribute very much to the low power consumption of the display.

As observed from Figure 6.10, the threshold voltage values are much higher in case of mixture **A**, **B** and **C** in comparison to mixture **D-G**. Since, mixture **D** comprises of only laterally fluorinated terphenyl derivatives it shows a moderate value of threshold voltage and in mixture **E** and mixture **F** in addition to the laterally fluorinated terphenyl derivatives, laterally fluorinated tolanes are also present, which results in lower values of threshold voltage. At T_{NI}–T=30°C the threshold values of mixtures **D**, **E** and **F** are around 2.43V, 1.98V and 2.67V respectively. Therefore, mixture **E** has the lowest value of V_{th} (~1.98V at around T_{NI}–T=30°C) among all of the mixtures studied. However, V_{th} values are slightly higher (~2.72 V at around T_{NI}–T=30°C) in case of mixture **G** due to the presence of bicyclohexane and non-mesogenic compounds.

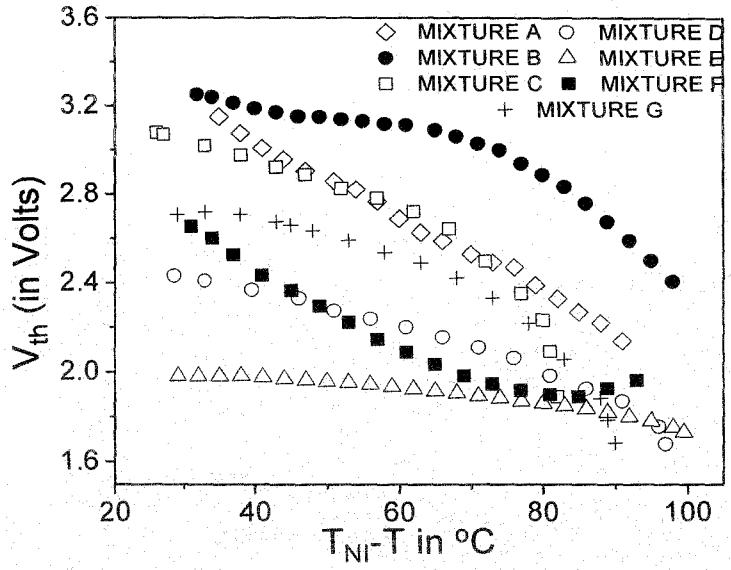

Figure 6.10. Threshold voltage values (V_{th}) as a function of relative temperature for different multicomponent mixtures (mixtures **A-G**). Key to symbols: ◊ mixture **A**, • mixture **B**, □ mixture **C**, o mixture **D**, Δ mixture **E**, ■ mixture **F** and + mixture **G**.

The temperature dependence of the bend elastic constant (K_{33}) for mixtures **A-G** are shown in Figure 6.11. The Freedericksz thresholds (V_{th}) [36, 37] for mixture **B** are slightly higher than those of **A**. The resultant effect is the reduced values of K_{33} for mixture **A** compared to mixture **B** [16]. It is found that the K_{33} values in mixture **A** is smaller in the entire nematic range compared to that of **B** [16]. A smaller elastic constant is favorable to achieve a low operating voltage, but it leads to a slower response time, because the response time is proportional to $1/K_{33}$. In practical cases, response time is usually more important than threshold voltage. Mixture **C** has a moderate K_{33} value of around 8.5 pN [15] at around 20°C. Mixtures **D, E** and **F** have higher values of K_{33} while for mixture **G** the same is slightly lower due to lower value of threshold voltage (V_{th}).

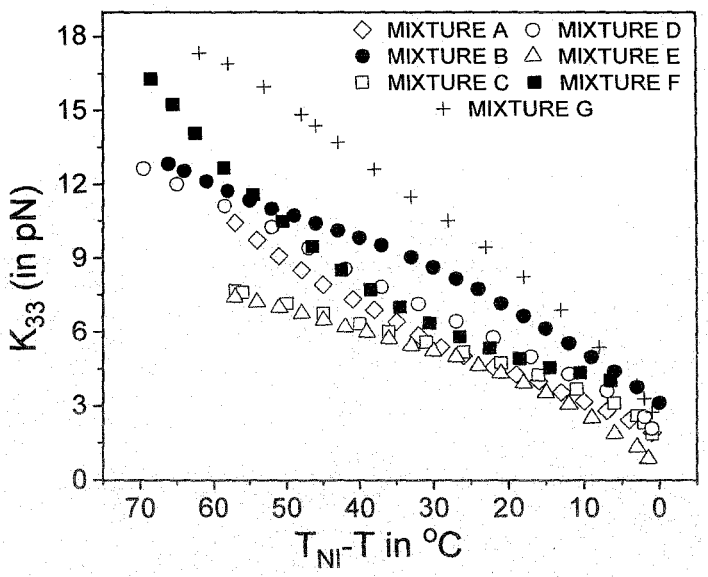

Figure 6.11. Bend elastic constant (K_{33}) as a function of relative temperature for different multicomponent mixtures (mixtures **A-G**). Key to symbols: ◊ mixture **A**, • mixture **B**, □ mixture **C**, o mixture **D**, Δ mixture **E**, ■ mixture **F** and + mixture **G**.

The elastic constant K_{33} is related to the nematic order parameter ($\langle P_2 \rangle$) by the relationship [35]:

$$K_{33} = A_0(\langle P_2 \rangle)^2 \qquad (6.6)$$

where A_0 is a material constant. As discussed in section 6.2.1, the temperature dependence of Orientational Order Parameter ($\langle P_2 \rangle$) has already been determined and these values along with the bend elastic constant values (K_{33}) are used in equation 6.6. Figure 6.12-6.13 shows the relationship between K_{33} and $(\langle P_2 \rangle)^2$ for the mixtures and confirms that the experimental results reported here are well fitted to equation 6.6. Similar behaviour has also been reported elsewhere [38]. The values of the material parameter A_0 for mixtures are listed in Table 6.2. The best agreement is obtained with the simple mean field prediction of Nehring and Saupe [39] that K_{33} is proportional to $(\langle P_2 \rangle)^2$. Largest value of A_0 is found for mixture **G** (around 35pN) and lowest value of

A_0 occurs for mixture **E** (around 21pN). The rest of the mixtures show a moderate value of this material parameter ranging in 25pN-31pN.

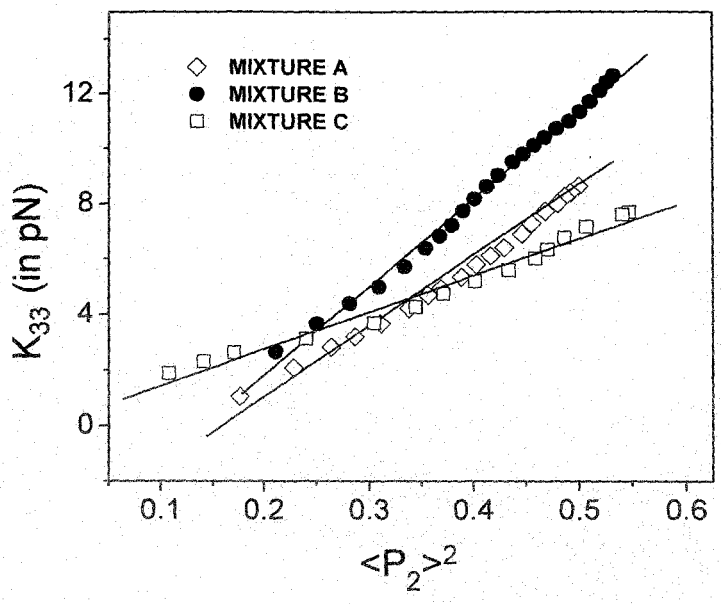

Figure 6.12. Validation of elastic constant $K_{33}=A_0\langle P_2\rangle^2$ for mixtures **A**, **B** and **C**. Key to symbols: o mixture **A**, • mixture **B** and □ mixture **C**.

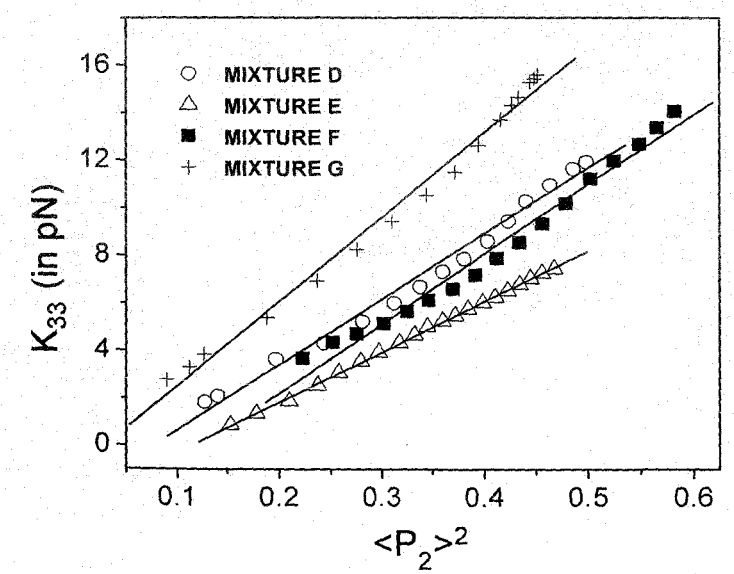

Figure 6.13. Validation of elastic constant $K_{33}=A_0\langle P_2\rangle^2$ for mixtures **D**, **E**, **F** and **G**. Key to symbols: o mixture **D**, Δ mixture **E**, ■ mixture **F** and + mixture **G**.

Table 6.2. Material parameter (A_0) values for mixtures **A-G** in pN.

Mixtures	Material parameter (A_0) in pN
A	25.52
B	31.85
C	23.36
D	27.54
E	21.15
F	29.29
G	35.51

6.2.4. Relaxation time (τ_0) and rotational viscosity (γ_1) measurements:

A simple electro-optical method [40-43, 15, 16] was used to determine the relaxation time and hence the rotational viscosities (γ_1) of all the multicomponent mixtures (mixture **A-G**). Studies of these parameters are most significant since this directly affects the quality of display devices.

Figure 6.14 shows the temperature dependence of relaxation time, τ_0. for all the mixtures **A-G**. Both the relaxation time (τ_0) and bend elastic constant values (K_{33}) were used to calculate the rotational viscosity of the mixtures **A-G**. The relaxation time for **B** is slightly lower than that of **A** [16]. However, the rotational viscosity of mixture **A** is slightly lower compared to that of mixture **B**. But, far away from the clearing temperature, the two values are close to each other. The response time for mixture **C** is 96 milisec and the rotational viscosity is 95mPas [15] at around 20°C. The laterally fluorinated terphenyl compounds are most promising components in mixtures which effectively lower the values of relaxation time and also the rotational viscosity [20, 21].

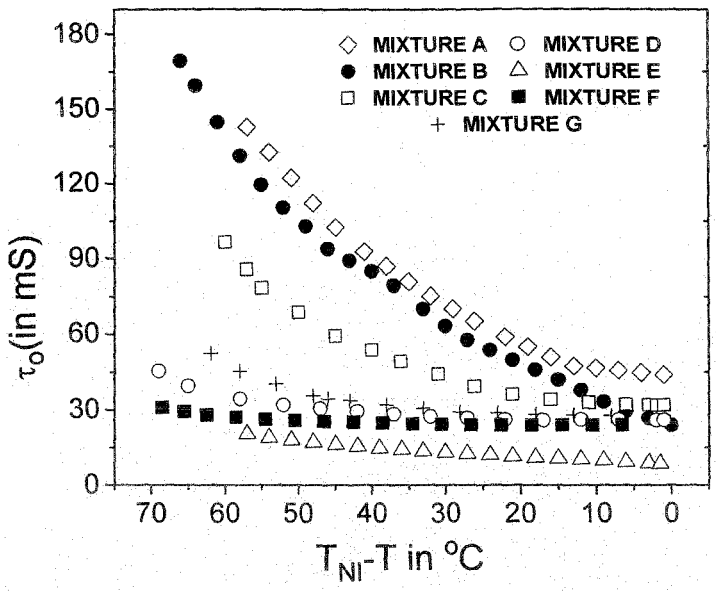

Figure 6.14. Relaxation time (τ_0) as a function of relative temperature for different multicomponent mixtures (mixtures **A-G**). Key to symbols: ◊ mixture **A**, • mixture **B**, □ mixture **C**, o mixture **D**, Δ mixture **E**, ■ mixture **F** and + mixture **G**.

Since, mixture **E** comprises of laterally fluorinated terphenyl compounds, its τ_0 values are much less than other mixtures. Laterally fluorinated tolanes are also effective for decreasing the values of τ_0. As a result mixture **E** and mixture **F** show quite low values of τ_0 of around 31ms and 28ms respectively at 20° C. There is a drastic improvement in the values of γ_1 for mixtures **D, E** and **F** (around 55-70 mPas at T_{NI}-T=65°C). However for mixture **G,** τ_0 and γ_1 both have moderate values of 80 mS and 89 mPas at around 20°C. This may be explained by the presence of compounds **10** and **11** (CH_2-CH_2 linkage group with bicyclohexane in the rigid core resulting in a rotational hindrance) [20] in mixture **G**, which effectively enhances the relaxation time (τ_0) as well as rotational viscosity (γ_1) of the mixture in comparison to other mixtures (mixture **D-F**).

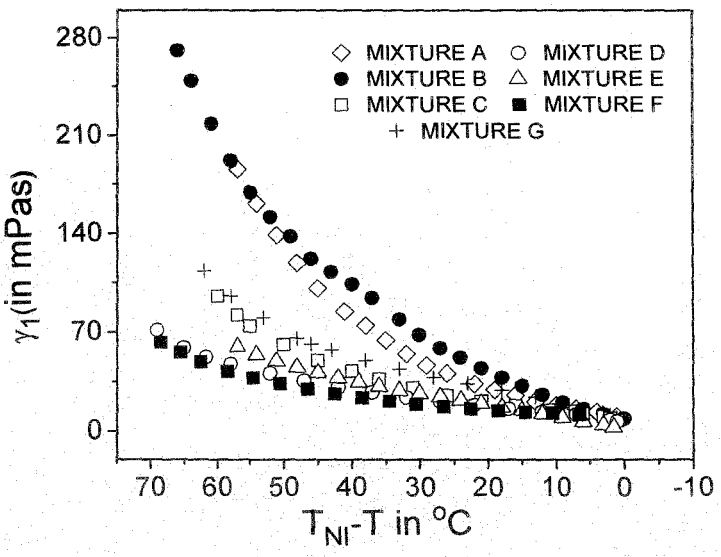

Figure 6.15. Rotational viscosity (γ_1) as a function of relative temperature for different multicomponent mixtures (Mixtures **A-G**). Key to symbols: ◊ mixture **A**, • mixture **B**, □ mixture **C**, o mixture **D**, Δ mixture **E**, ■ mixture **F** and + mixture **G**.

6.2.5. Activation Energy:

The temperature dependence of γ_1 is fitted with the following expression using the values of the orientational order parameter, $\langle P_2 \rangle$, obtained from birefringence measurement:

$$\gamma_1 = \gamma_0 \langle P_2 \rangle \exp\left(\frac{E_a}{k_\beta T}\right) \tag{6.4}$$

where γ_0 is the rotational viscosity at absolute zero temperature, k_β is the Boltzmann constant, $\langle P_2 \rangle$ is the Orientational Order Parameter (OOP) and E_a is the associated activation energy [17].

A systematic study of rotational viscosity and Orientational Order Parameter (OOP) has already been studied for all of the multicomponent mixtures (mixtures **A-G**). These values have been used further to calculate the activation energy (E_a) of the multicomponent mixtures (mixtures **A-G**) under investigation.

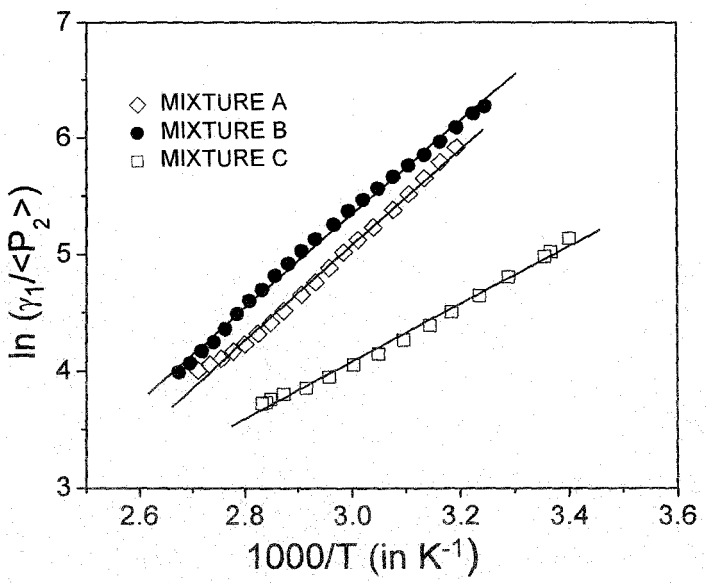

Figure 6.16. The Arrehenius plot for rotational viscosity (γ_1) related to the nematic phase for multicomponent mixtures **A**, **B** and **C**. Key to symbols: ◊ mixture **A**, • mixture **B** and □ mixture **C**.

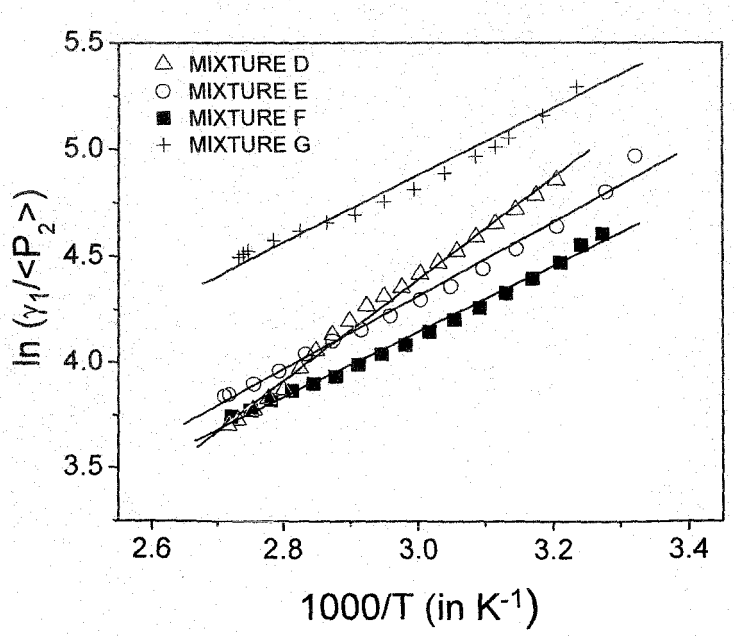

Figure 6.17. The Arrehenius plot for rotational viscosity (γ_1) related to the nematic phase for multicomponent mixtures **D-G**. Key to symbols: o mixture **D**, Δ mixture **E**, ■ mixture **F** and + mixture **G**.

The Arrhenius plot (ln $\gamma_1/\langle P_2 \rangle \sim 1/T$ plot) [35] in the nematic phase of the mixtures (mixture **A-G**) using the calculated values of the orientational order parameter ($\langle P_2 \rangle$) and rotational viscosity (γ_1) are shown in Figures 6.16 and 6.17. From the slope of the Arrehenius plot the activation energy E_a have been evaluated. The activation energies thus obtained for these multicomponent mixtures (mixture **A-G**) are given in Table 6.3.

Table 6.3. Activation energies (E_a) for mixtures **A-G** in kJ/mole.

Mixtures	**E_a in kJ/mole**
A	30.34
B	32.81
C	26.14
D	36.24
E	39.38
F	41.45
G	45.76

It can be concluded from the activation energy (E_a) data that mixture **C** has the lowest E_a value (26kJ/mole) while for the rest of the mixtures E_a values are higher (varies from 30-45kJ/mole) if compared with mixture **C**. This is expected since the temperature dependent rotational viscosity data are steeper at lower temperatures, contributing more to the slope of the Arrehenius plot. Actually the average value of E_a within the nematic phase is computed for these multicomponent mixtures. These mixtures have lower viscosity values and also have lower values of E_a. The dipole-dipole correlations may affect the values of E_a [17, 35].

6.2.5. Determination of Visco-elastic co-efficient (γ_1/K_{33}) and Figure of Merit (FoM):

The visco-elastic co-efficient (γ_1/K_{33}) [44] curves are shown in Figure 6.18 for mixtures **A-G** as a function of relative temperature. Mixture **B** shows the highest value of the visco-elastic coefficient (~60 at around room temperature) as rotational viscosity values are highest for this mixture, whereas the bend elastic constant values are moderate [16]. Mixtures **B** and **C**, with moderate values of both rotational viscosity and bend elastic constant has a moderate value of γ_1/K_{33} (around 20-30 in the nematic range) [15, 16]. However, mixtures **D-G** show very good performance as far as the visco-elastic co-efficient values are concerned (~ 5-15 at around room temperature) as their rotational viscosity values are very low in comparison to mixtures **A-C**, but bend elastic constant values are moderate.

Figure 6.19 illustrates the FoM curves [44] for mixtures **A-G** as a function of relative temperature. As expected, mixtures **A-C** have lower FoM values since their rotational viscosity values are higher than mixtures **D-G**. The peak values are around 1.3-1.8 $\mu m^2/s$ for mixtures **A-C**. For mixture **D**, the peak value is around 13 $\mu m^2/s$, while for mixtures **E**, **F** and **G** the peak values are around 7-9 $\mu m^2/s$. Based on the direct FoM comparison of the investigated LC mixtures, it is concluded that the mixtures consisting of laterally fluorinated two and three phenyl rings compounds are more favorable for room temperature operation in display devices. The advantages are twofold: lower viscosity and higher birefringence. Thus for the mixtures intended for an elevated temperature operation, some compounds, e.g., cyclohexane or tolanes, with a high clearing temperature should be incorporated (mixture **E** and mixture **F**) in order to improve the clearing temperature.

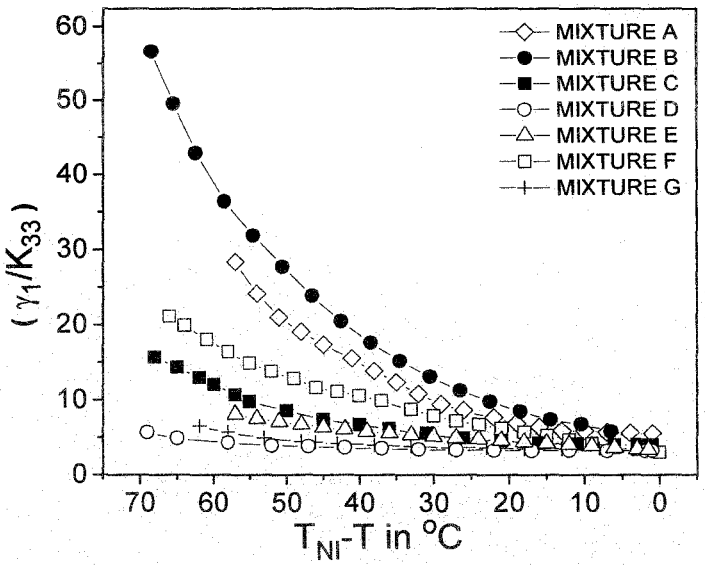

Figure 6.18. Visco – elastic ratio (γ_1/K_{33}) as a function of relative temperature for different multicomponent mixtures (mixtures **A-G**). Key to symbols: ◊ mixture **A**, • mixture **B**, □ mixture **C**, o mixture **D**, Δ mixture **E**, ■ mixture **F** and + mixture **G**.

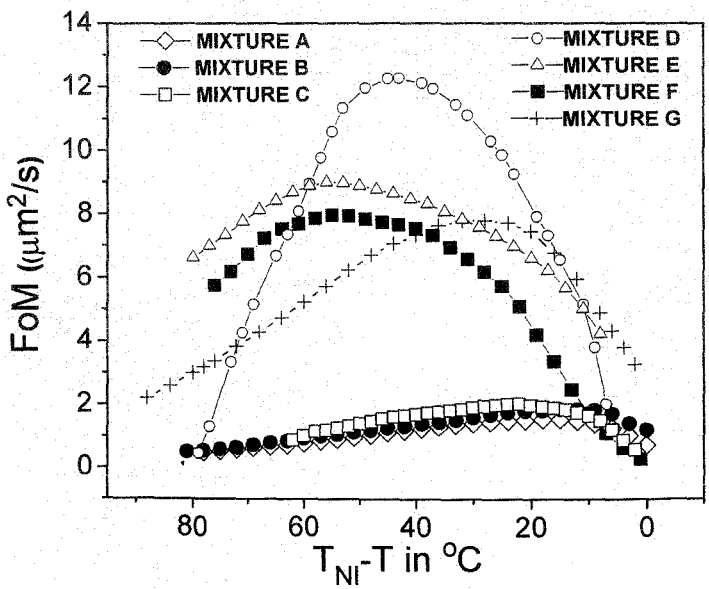

Figure 6.19. Figure of Merit (FoM) as a function of relative temperature for different multicomponent mixtures (mixtures **A-G**). Key to symbols: ◊ mixture **A**, • mixture **B**, □ mixture **C**, o mixture **D**, Δ mixture **E**, ■ mixture **F** and + mixture **G**.

6.3. Comparative study:

The physical properties of the seven multicomponent mixtures (mixtures **A-G**) have been extensively studied. The physical properties of these mixtures **A-G** have been compared in Table 6.4. All of them are eutectic mixtures and it is observed that mixtures **D**, **E** and **F** emerged as moderately good mixtures for VA mode liquid crystal displays from application point of view.

Table 6.4. Comparison of the physical properties of the multicomponent mixtures (mixtures **A-G**) (at ~ 20°C).

	A	**B**	**C**	**D**	**E**	**F**	**G**
T_{NI}	97.5°C	100.5°C	80.9°C	105.9°C	110.5°C	107.4°C	96.0°C
T_m	11.7°C	15.4°C	–5.3°C	–13.4°C	–14.8°C	–14.5°C	–27.2°C
Δn	0.12	0.12	0.11	0.19	0.18	0.18	0.19
$\Delta\varepsilon$	–1.4	–1.2	–0.9	–2.4	–2.9	–2.3	–2.6
V_{th} (in volts)	3.33	3.18	2.82	2.38	2.33	3.19	2.07
K_{33}(in pN)	14.47	13.54	8.20	14.35	14.63	13.74	14.39
τ_0 (in milisec)	164	218	72	25	31	28	32
γ_1 (in mPas)	464.1	440.9	124.1	47.7	55.8	57.3	71.9

6.4. Summary and Conclusions:

Based on the results of the physical parameters of individual compounds as described in Chapter III, several multi-component mixtures (mixture **A-G**) had been formulated. Laterally fluorinated bi-phenyl and tri-phenyl compounds, laterally fluorinated tolanes, two bicyclohexane compounds and also two non-mesogenic compounds were used to formulate the mixtures and their compositions were given in Chapter V. The purpose of preparing and characterizing these mixtures was to get best multicomponent mixture with

excellent electro-optical performance to be used in VA mode displays. The physical properties of all of the negative dielectric anisotropy nematic liquid crystalline multicomponent mixtures (mixture **A-G**) have been investigated by different experimental techniques and birefringence (Δn), dielectric anisotropy ($\Delta\varepsilon$), bend elastic constant (K_{33}), relaxation time (τ_0) and rotational viscosity (γ_1) had been determined. The order parameter ($\langle P_2 \rangle$) values have been calculated. In addition to these the visco-elastic co-efficient (γ_1/K_{33}) and FoM values have been evaluated.

In the tri component mixtures (mixtures **A** and **B**), the optical birefringence were found to almost satisfy the targeted values for VA mode display devices (around 0.11) but $\Delta\varepsilon$ values are too low (~ −1 at around 20°C). To meet this requirement five component (mixture **C**) and nine component (mixture **D**) mixtures were prepared. For mixture **D** low viscosity (~ 48 mPas at around 20°C) and moderate birefringence (~ 0.18 at around 20°C) and higher values of dielectric anisotropy (~ −2.5 at around 20°C) with a broad nematic range had been achieved. By introducing two different dopants (laterally fluorinated tolanes) the nine component mixture has been modified into two ten component mixtures (mixtures **E** and **F**) where almost all the physical properties were tailored to meet the required specification of the display material, only with a slight deviation in the birefringence (Δn) values. The fifteen component mixture (mixture **G**) gave a reasonable balance among all the required physical properties for a suitable VA display device. Mixtures **D-F** emerged to be the best mixture among all the mixtures studied.

References:

[1] T. Sugiyama, Y.Toko, T. Hashimoto, K. Katoh, Y. Limura, S. Kobayashi, *J.Phys. D:Applied Physics.*, ***8***, 1575 (1975).

[2] M.F. Schiekel and K. Fahrenschon, *Appl. Phys. Letts.*, ***19(10)***, 391 (1971).

[3] S.H. Hong, Y.H. Jeong, H.Y. Kim, H.M. Cho, W.G. Lee and S.H. Lee, *J. Appl. Phys.*, ***87***, 8259 (2000).

[4] S.C.A. Lien, C. Cai, R.W. Nunes, R.A. John, E.A. Galligan, E. Golgan and J.S. Wilson, *Jpn. J. Appl. Phys.*, ***37***, 597 (1998).

[5] S.M. Kelly and M.O'Neill, *Handbook of Advanced Electronic and Photonic Materials and Devices, Vol. 7, Academic Press*. Chapt. 1 (2000).

[6] D.K. Yang and S.T. Wu, *Fundamentals of Liquid Crystal Devices*, John Wiley & Sons, Chapt. 8 (2006).

[7] S. Shimizu, Y. Ochi, A. Nakano and M. Bone, *Soc. Info. Disp. Symp. Digest. 72* (2004).

[8] H.M. Chen, K.Q. Zhao, L. Wang, P. Hu, B.Q. Wang, Soft Mater ***9***, 359 (2011).

[9] S.Ghosh, P.Nayek, S.K. Roy, T.P.Majumder and R.Dabrowski, *Liq. Cryst.*, ***37***, 369 (2010).

[10] M.R. Cargilla, G. Sandforda, A.J. Tadeusiaka, G.D. Loveb, N. Hollfelderc, F. Pleisc, G. Nellesc and P. Kilickiranc, *Liq. Cryst.*, ***38***, 1069 (2010).

[11] J.W. Goodby, *Liq. Cryst.*, ***38***, 1363 (2011).

[12] D. Pauluth and K. Tarumi, *J. Mater. Chem.*, ***14***, 1219 (2004).

[13] Y.M. Zhang, D. Wang , Z.C. Miao, S.K. Jin and H. Yang, *Liq.Cryst.*, ***39(11)***, 1330 (2012).

[14] D. Pauluth and K. Tarumi, *J. SID*, ***13***, 693 (2005).

[15] P. Dasgupta, B. Das and M.K. Das, *Liq. Cryst.*, ***39 (11)***, 1297 (2012).

[16] S. Basak, P. Dasgupta, B. Das, M.K. Das and R. Dabrowski, *Acta Physica Polonica A.* ***123(4)***, 714 (2013).

[17] W.H. de Jue, *Physical Properties of Liquid Crystalline Materials;* Gordon and Breach Science Publishers: London, (1980).

[18] A.K. Zeminder, S. Paul and R. Paul, *Mol. Cryst. Liq. Cryst.*, ***61***, 191 (1980).

[19] A. Prasad and M. K. Das, *Phase Transitions*, ***83***, 1072 (2010).

[20] D.A. Dunmur, A. Fukuda and G.R. Luckhurst, *Physical Properties of Liquid Crystal Nematics*, INSPEC publications, London, U.K. (2001).

[21] M. Hird, *Chem. Soc. Rev.*, ***36***, 2070 (2007).

[22] M. Hird and K.J. Toyne, *Mol. Cryst. Liq. Cryst.*, ***323***, 1 (1998).

[23] I. Haller, H.A. Huggins, H.R. Lilienthal and T.R. McGuire, *J. Phys. Chem.*, *77*, 950 (1973).

[24] I. Haller, *Prog. Solid State Chem.*, ***10***, 103 (1975).

[25] M.F. Vuks, *Optics and Spectroscopy*, ***20***, 361 (1966).

[26] H.E. Neugebauer, *Canad. J. Phys.*, **32**, 1 (1954).

[27] W. Kuczynski, B. Zywucki, and J. Malecki, Mol. Cryst. Liq. Cryst. **381**, 1 (2002), and references cited therein; M. Ramakrishna *et al.*, *ibid.* **528**, 49 (2010).

[28] M.K. Das, A Pramanik, B. Das, Ł Szczuciński and R Dabrowski, *J. Phys. D: Appl. Phys.*, ***45***, 415304 (2012).

[29] P.D. Roy, A. Prasad and M.K. Das, *J. Phys.: Condens. Matter.*, ***21(7)***, 075106 (2009).

[30] A. Prasad and M.K. Das, *J. Phys.: Condens. Matter.*, ***22***, 195106 (2010).

[31] M.K. Das, G. Sarkar, B. Das, R. Rai and N. Sinha, *J. Phys.: Condens. Matter.*, ***24***, 115101 (2012).

[32] A. Chakraborty, B. Das, M.K. Das, S. Findeisen-Tandel, M.G. Tamba, U. Baumeister, H. Kresse and W. Weissflog, *Liq. Cryst.*, ***38(9)***, 1085 (2011).

[33] V. Reiffenrath, J. Krause, H.J. Plach and G. Weber, *Liq. Cryst.* ***5***, 159 (1989).

[34] C. Housecroft, E. Catherine and A.G. Sharpe, *Inorganic Chemistry.*, 3rd Edn. Harlow: Pearson Education (2008).

[35] B. Bahadur, *Liquid crystals: Applications and Uses*, World Scientific: Singapore, Vol. I (1991).

[36] V. Freedericksz and V. Tsvetkov, *Phy. Z. Soviet Union*, ***6***, 490 (1934).

[37] V. Freedericksz and V. Zolina, *Trans. Faraday Soc.*, ***29***, 919 (1933).

[38] A. Pramanik, B. Das, M.K. Das, K. Garbat, S. Urban and R. Dabrowski, *Liq. Cryst.*, ***40***, 149 (2013).

[39] J. Nehring and A. Saupe, *J. Chefit. Phis.*, ***56***, 5527 (1972).

[40] S. T. Wu and C. S. Wu, *Phys. Rev. A*, ***42***, 2219 (1990).

[41] M. L. Dark, M. H. Moore, D. K. Shenoy and R. Shashidhar, *Liq. Cryst.*, ***33***, 67 (2006).

[42] M. K. Das, A. Pramanik, B. Das, L. Szczucinski and R. Dabrowski, *J. Phys. D: Appl. Phys.*, ***45***, 415304 (2012).

[43] A. Chakraborty, M. K. Das, B. Das, A. Lehmann and C. Tschierske, Soft Matter, **9**, 4273 (2013).

[44] S. Gauza, M. Jiao, S.T. Wu, P. Kula, R. Dabrowski and S. Liang, *Liq. Cryst.*, ***35(12)***, 1401 (2008).